EuroSun2026

SOLAR DISTRICT HEATING NETWORK WITHOUT BIOMASS: SUPPLYING HEAT TO A RURAL VILLAGE

Christoph Schmelzer, Paul Volk, Oleg Kusyy, Klaus Vajen

University of Kassel / Department of Solar and Systems Engineering, Kassel (Germany)

solar@uni-kassel.de

Summary

Decarbonizing the heat supply of existing residential buildings remains one of the key challenges of the energy transition in Germany and across Europe. In rural settlements with predominantly single-family homes, the transformation of individual heating systems is often very slow due to low renovation rates and high investment costs. Here, solar district heating networks with seasonal thermal energy storage offer a promising pathway for achieving high shares of renewable heat while maintaining economic feasibility. This paper presents the innovative solar district heating project under construction in Rüdigheim (Hesse, Germany), designed to supply around 100 households with 2.3 GWh/a climate-neutral heat via a approx. 5 km heating network. The system combines a large-scale solar thermal collector field (approx. 5.500 m²) with a seasonal storage (TTES 17,400 m³) and an internal heat pump to maximize storage capacity and system efficiency. The system aims to achieve an exceptionally high solar fraction of approximately 87 %, making it one of the highest solar shares implemented in a district heating system worldwide.

solar district heating, seasonal thermal energy storage, rural heat transition, renewable heat

Field of application for the findings: Renewable district heating systems, rural energy systems

Addressed audience: Researchers, planners, municipalities, utilities, and policy makers

1. Introduction

Space heating is one of the largest sources of greenhouse gas emissions from buildings in Europe. Decarbonizing space heating is essential for the EU to reach climate neutrality by 2050 (EU, 2021). Germany has set this goal already for 2045 (Deutscher Bundestag, 2019). In dense, urban areas, district heating networks, which combine heat pumps, thermal storage, and diverse renewable or waste heat sources within a low-temperature network, are widely regarded as a central pathway toward this goal. These networks increase the share of renewable energy and the flexibility of the heat supply (Lund et al., 2014; Werner, 2017), while pooling investment across many buildings to lower overall system costs (Mathiesen et al., 2015; Brown et al., 2018). In rural areas where heat densities are typically low, however, the heat transition mainly relies on individual building renovations and installing decentralized (air to water) heat pumps. Since renovation costs are high relative to the relatively low building values, the renovation rates are low, resulting in a slow heat transition (Gerhardt, 2019; Buildings Performance Institute Europe, 2022). A renewable district heating network can avoid this bottleneck. Heat is decarbonized centrally rather than building by building. Because land for pipes, energy centers, and large collector or storage areas is comparatively cheap in rural areas, the resulting cost savings can offset the disadvantage of lower heat density typical of rural settlements. This option is further strengthened by dedicated public funding for efficient heating networks (Bundesamt für Wirtschaft und Ausfuhrkontrolle (BAFA), 2022).

Many rural district heating networks currently rely on biomass, using locally available wood chips or biogas to supply cost-competitive, CO_2-neutral heat at today's prices (Soltero et al., 2018). This dependence carries risks, however: combustion causes local air pollution (Steiner and Lanzerstorfer, 2024), and rising demand from other heating networks as well as from industry and transport may drive biomass prices up (Harrandt et al., 2025) or ultimately make its supply unsustainable (Pozo et al., 2024). Solar thermal energy offers a way to reduce this dependence, particularly in summer, when research initiatives such as the IEA SHC programme (IEA SHC, 03.12.2025) and IEA SHC Task 68 (IEA SHC Task 68, 01.12.2025) identify it as one of the most cost-effective renewable heat sources for district heating. Heat pumps could, in principle, cover the remaining share of the year as well (Lepiksaar et al., 2021), but their year-round operation adds considerable load to the electricity grid, particularly in winter (Damianakis et al., 2023).

Seasonal thermal energy storage has the opportunity to capture solar heat in summer for use throughout the winter, allowing a large share of the annual heat demand to be generated onsite, rather than using biomass, gas or grid electricity. Large pit (PTES) or tank (TTES) thermal energy storages are becoming increasingly affordable, are already operating at scale mainly in Denmark, and are the subject of active research such as IEA Energy Storage Task 39 (IEA ES Task 39, 01.12.2025) and Task 45 (IEA ES Task 45, 21.11.2025) or the European TREASURE project, which aims to scale up pit storages further (TREASURE Project, 21.11.2025). Combined with seasonal storage, solar district heating has been shown to reach very high renewable shares. Braimakis et al. (Braimakis (2025)) find that low-temperature networks can be supplied entirely from solar energy in Athens and still reach solar fractions of 50–60 % in Munich or Copenhagen, mainly depending on collector area and storage volume, while Kelch et al. (2024) show that, even for older rural buildings, such a system can be economically competitive with individual heat-pump renovations while reaching solar fractions of around 70 %. On the other hand, studies such as Trabert et al. (2020) still find a biomass-supported solution cheapest for a German village, and Słomczyńska et al. (2022) show that charging a large pit storage with solar thermal collectors requires less space and investment than a photovoltaic alternative, though without accounting for its costs over the full storage lifetime.

The village of Amöneburg-Rüdigheim, in Hesse, Germany, is a representative example of the rural settlements addressed above. 90 % of its buildings were built before 1980 and or even half-timbered, making them particularly costly to renovate, while heat is currently supplied almost entirely by individual oil and gas boilers (see Figure 1). To reach carbon neutrality in heating, a solar district heating network is currently under construction in Rüdigheim that combines a large solar collector field with a seasonal thermal storage and an internal heat pump. Unlike most other solar district heating networks, it does not rely on any biomass at all, aiming to supply around 100 buildings at an exceptionally high solar fraction. The following sections present the resulting system concept, its current construction status and an outlook for the project.

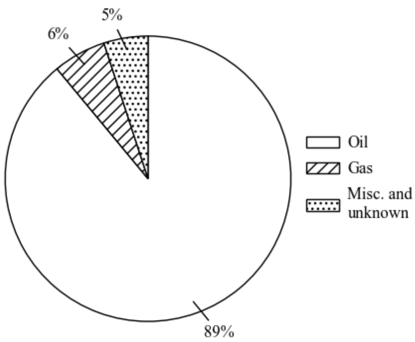

Fig. 1: Current shares of the heat supply in Rüdigheim.

2. From Concept to Implementation-Ready Design

The plan for a renewable district heating network in Amöneburg-Rüdigheim originated from a citizens' co-operative that aimed to supply the village entirely from solar energy, avoiding both biomass and the price volatility of fossil fuels. A planning office, together with a plant constructor and a manufacturer of tank thermal energy storages (TTES), translated this goal into an initial concept comprising a 7,000 m^2 field of evacuated tube collectors and two 15,000 m^3 seasonal storage tanks, intended to connect around 100 of the village's buildings(Volk et al., 2025). Figure 2 shows the resulting layout of the heating network. The storage, energy central and collector field are located on the outskirts of the village.

Fig. 2: Layout of the Rüdigheim heating network. DHN marked in red, connected houses in green, seasonal storage and collector field in yellow.

As the state subsidies assumed in this initial concept no longer applied and the associated cost estimates had to be revised, the University of Kassel, supported by the Hesse State Energy Agency (LEA: Landesenergieagentur Hessen), joined the project to verify its technical and economic feasibility. The manufacturer's system model was transferred to TRNSYS and coupled with the optimization tool GenOpt to systematically resize the main components for the lowest levelized cost of heat (Volk et al., 2025). The manufacturer could not supply a single storage tank larger than 15,000 m^3, so the resulting implementation-ready design uses only one such tank instead of two for cost reasons, even though a larger storage volume would have increased the solar fraction at same cost. The TTES in this initial concept is discharged by an internal heat pump that cools its lower layers below the 40 °C network return temperature and feeds it back to the TTES at supply temperature to increase the usable storage capacity. To keep the collector field affordable despite the reduced storage volume, flat-plate collectors are connected in series ahead of the evacuated tube collectors (ETC), preheating the fluid before it is reheated to the required supply temperature in the evacuated tube collectors. Table 1 summarizes the resulting boundary conditions, which achieved a solar fraction of about 87 % and formed the direct basis for the system now under construction (Figure 3).

Tab. 1: Boundary conditions of the implementation-ready concept identified by Volk et al. (2025).

Parameter	Value
Heat demand	2.3 GWh/a
Connected buildings	approx. 100
Network length	5.4 km
Network supply / return temperature	68 °C / 40 °C
Collector field (total / FPC / ETC)	5,700 m^2 (4,400 m^2 / 1,300 m^2)
Seasonal storage volume	15,000 m^3 (1 concrete tank)
Internal heat pump, thermal capacity	approx. 1 MW$_{th}$
Solar fraction	87 %

Additionally, the first study simulated and optimized the system using current (2020) weather data from Meteonorm 7. However, during the planning phase, it became apparent that the solar radiation values in this data differed significantly from those in Meteonorm 8. It is more logical to use weather data for the future, given that the system will be operational at that time. Meteonorm 8's monthly average solar radiation values for 2030 (normal year, RCP2.6) are up to 40 % higher than Meteonorm 7's values for 2020. This means that different collector sizing options become possible. However, this effect is countered by the preliminary study's assumption that there would be sufficient space for the collectors to operate year-round without shading and facing south. Changes in the framework conditions, however, have revealed that the available area for collectors is limited to 12,000 m^2, and only 60 % of this area can be used. Therefore, shading cannot be prevented. Furthermore, the available area is not entirely oriented toward the south, but rather at an angle of approximately 30° toward the southeast, which increases shading.

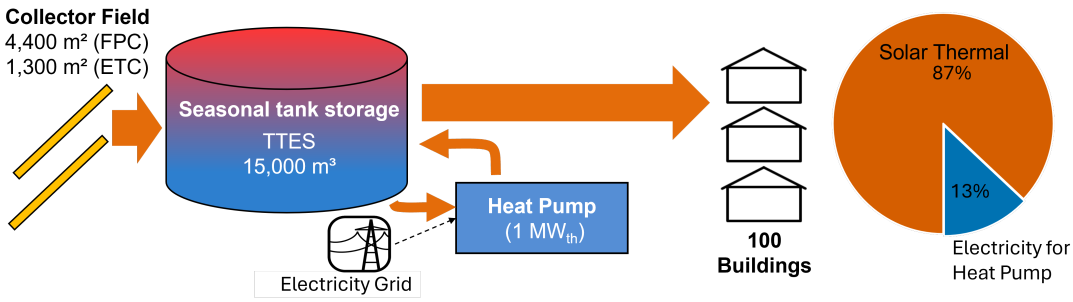

Fig. 3: Favored concept resulting from the 2024 optimization study based on the boundary conditions in Table 1 (Volk et al. (2025)).

3. New Boundary Conditions in Realization-Phase

3.1 Changes in the system boundary conditions

Based on these new boundary conditions, further design optimizations were ultimately carried out. Additionally, several changes were applied to the original design parameters used to size and optimize the concept before construction of the facility began. For instance, it was now possible to use a steel-framed TTES, which resulted in a maximum volume of around 17,400 m³ (any larger volume would have required a new building permit). This higher volume was the implemented, since the pre-design studies indicated a higher TTES volume as cost-beneficial. Due to cost considerations and a lack of offers from manufacturers, the concept of a mixed collector field consisting of flat-plate and evacuated-tube collectors was not pursued. Consequently, only one of the two technologies could be used. The limited available land space of approximately 12,000 m² posed the additional challenge of generating enough solar heat to fully fill the larger storage tank under these new constraints. Due to rising interest rates and higher costs compared to the original plan, it was also necessary to find a configuration that would minimize investment costs. For these reasons, additional simulations were conducted to determine how the heat pump could be designed smaller. Moreover, alternatives to the specialized building transfer stations were investigated, as the stations identified in the original studies incurred particularly high investment costs. The drawback of this was that slightly higher return temperatures now had to be anticipated. In summary, the challenge was to find a configuration that would allow for a larger storage tank, higher return temperatures, and the smallest possible heat pump within a limited space, while still supplying the village primarily with solar heat and without using biomass or gas boilers.

Since the DHN in Ruedigheim only uses solar heat and an internal heat pump, special focus was placed on the weather data as well. To estimate the impact of different irradiation scenarios and ambient temperatures on the system performance, the simulations were conducted with P10, P50 and P90 weather data for 2030 from Meteonorm 8. Especially the P90 weather data is relevant for the following sizing of the heat pump, since it represents a cold winter scenario with low solar irradiation.

3.2 Improvement of the control strategy

First, the model was adjusted to the new boundary conditions in the TRNSYS simulations. This included the new TTES volume of 17,000 m³ and an adjusted return temperature of 45 °C. Additionally, the control strategy for winter and summer were adjusted. Figure 4 displays the improved control strategy for the heating network in winter. The volume in the upper storage section was adjusted to a holding temperature of 75 °C. This allows the system to better cover peak loads and requires a lower heat pump capacity. The heat pump can "prepare" in advance, so it no longer has to immediately compensate for every peak load. In the model, the heat pump was configured to allow a maximum evaporator temperature of 50 °C. It cools the storage water by 5 K and maintains the temperature of 50 °C until it can no longer be sustained. Consequently, the heat pump can only activate once the storage tank reaches 50 °C. Until then, the grid load is covered directly, without the use of the heat pump. Then, the heat pump cools the lower portion of the storage tank until the end of the heating season.

On the condenser side, the available connections mix an inlet temperature of 65 °C, which is then increased by 10 K to the temperature of the standby volume. In winter, the solar thermal system also operates at a lower temperature to achieve higher yields. It then serves only to preheat the heat pump. In doing so, it continuously feeds the top third of the storage tank with the current temperature. If this temperature falls below 50 °C, the system continues to operate with a solar thermal flow temperature of 50 °C for the remainder of the winter.

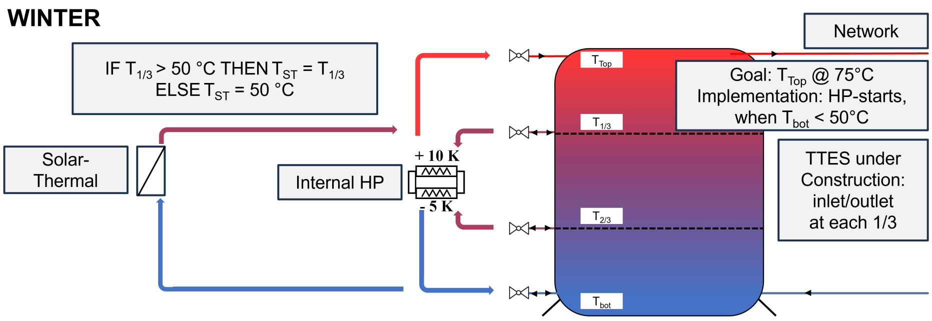

Fig. 4: Improved control strategy for the Rüdigheim district heating network in winter to maximize collector yield.

The simulation also involved testing operating strategies for the summer with the goal of further increasing collector output (see Figure 5). After the heating season ends and the storage tank reaches its lowest temperature, the primary goal is to avoid using the heat pump to minimize external energy input and reduce operating costs. This is accomplished by first heating the top third of the storage tank to a temperature of 75°C (system supply temperature plus 5 K), meaning the solar thermal system initially operates at 75°C (Mode 1). Then, the solar thermal system is fed by the cooler layer at $T_{2/3}$ to heat the upper two-thirds of the storage tank to the holding temperature of 75 °C (Mode 2). The solar thermal system only operates at the storage tank's maximum temperature of 95 °C and fully charges the tank (Mode 3) once this has been achieved, in order to minimize the time spent in temperature ranges that are unfavorable for the solar thermal system throughout the year.

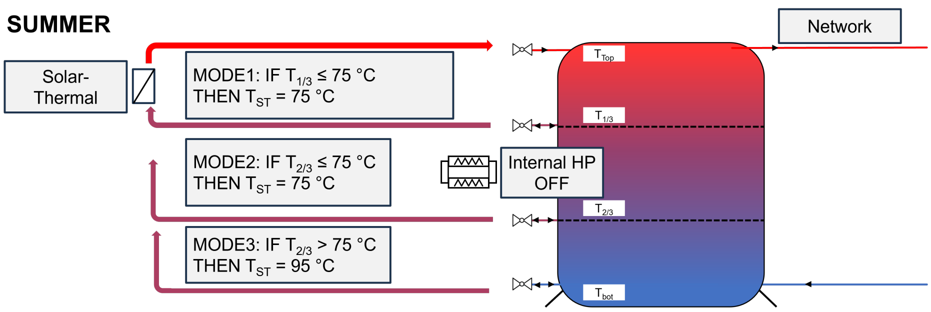

Fig. 5: Improved control strategy for the Rüdigheim district heating network in summer to maximize collector yield.

3.3 Simulation results with new boundary conditions

With the aforementioned adjustments, the system configurations were again simulated and optimized for the lowest levelized cost of heat in the first step with average weather data (P50). Collector technology (flat plat and evacuated-tube), collector area and tilt angle were varied automatically to find the optimal configuration. The optimization results were discussed with industry and project partners to identify the most promising configuration for the Rüdigheim district heating network. The discussion yielded the following configuration. A preliminary field size of 5,500 m^2 evacuated-tube collectors was chosen, which is approximately the maximum size that can be installed on the available land. With this set field size, simulations were conducted to determine the minimal heat pump capacity required to cover the heat load in winter for P90-conditions, to minimize necessary investment and therewith LCoH. This resulted in a heat pump capacity of 770 kW$_{th}$ (nominal, maximum output approx. 1,000 kW$_{th}$).

Figure 6 shows the energy balances for each month and the solar fraction for the final configuration and P50 weather data. It can be seen that the overall solar fraction is decreased to 83 % compared to the original configuration due to a smaller collector field and consequently higher electricity input. However, with this configuration, about 150,000 EUR of investment costs can be saved (700 EUR/kW for heat pump capacity were given by industry partners). Of course, this results in higher electricity costs during the operation period, but this is accepted since this change is primarily motivated by the restricted available land area and the subsequently limited collector area. The monthly energies show that there is very little solar thermal input for December and

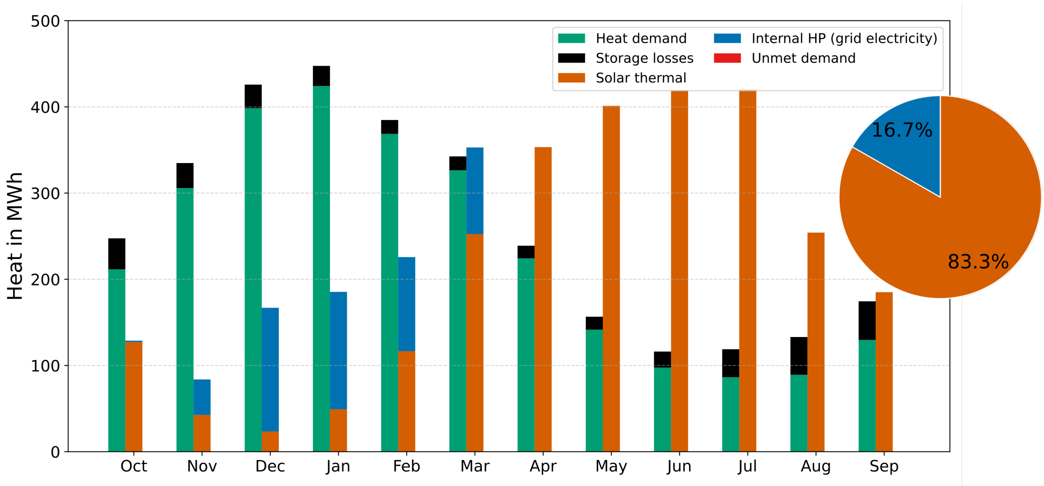

Fig. 6: Energy balances and solar fraction for the final system configuration with 5,500 m^2 evacuated-tube collectors and a 770 kW_{th} internal heat pump.

January, while the solar production peaks at June and July at approximately 450 MWh/month. In August the solar energy yield is already reduced significantly, due to the limited storage capacity. The heat pump starts supplying heat in November and operates almost continuously until March, with a peak electricity input in January at about 135 MWh. The operation in March is mainly due to a cold spell in the P50 weather data, which cannot be covered by stored energy and solar thermal input alone at that point. The seasonal storage losses accumulate to about 300 MWh/year, which is about 10 % of the total energy input.

4. Air as an Additional Heat Source for Internal HP: Potential Cost Savings

Due to the increased overall investment costs during the planning phase, additional technology combinations were investigated. Since the original concept already incorporated a (booster) heat pump, the idea arose to use the ambient air as an additional heat source for the internal heat pump in summer, combined with a PV field to directly supply the necessary electricity. Operating the heat pump only on PV electricity also supports the system's main goal of a high solar fraction. The size of the internal heat pump was kept the same as in the previous optimization for minimal investment costs, this ensured that the operation strategy in winter did not need to be adjusted. In order to use air as an additional heat source in summer, an additional fluid loop is required between the air-water heat exchanger and the evaporator of the internal heat pump. An approach temperature of 5 K was assumed for the heat transfer between the ambient air and the source-side inlet temperature.

4.1 Adapted Control Strategy for System with AHP Addition

The adapted control strategy for summer is shown in Figure 7. The winter control strategy overall and the solar thermal control for summer remains is unchanged, but now the heat pump can use outdoor air as additional heat source, if the ambient temperature is above 10 °C. The heat pump is used here to preheat the lower third of the seasonal storage up to the heat pump's maximum temperature of 75 °C. Additionally, the heat pump only operates when the PV field can supply enough electricity to meet the heat pump's electricity demand. It is assumed that the heat pump can modulate down to 25 % of its nominal capacity, allowing for a more flexible operation and better matching of the PV electricity supply.

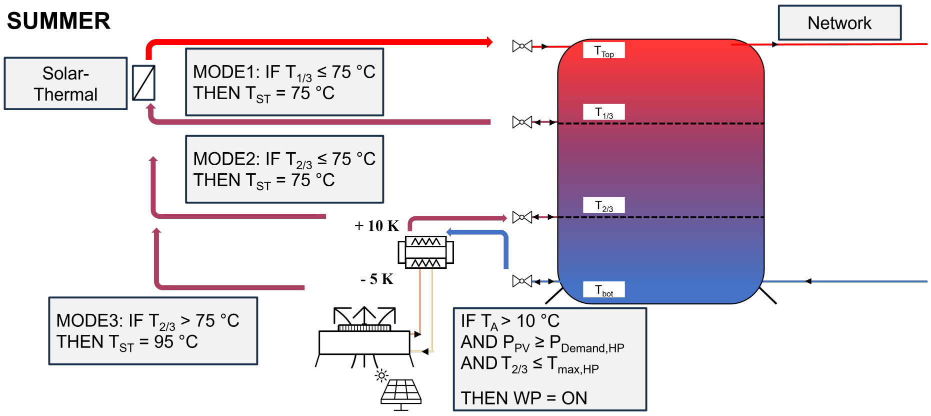

Fig. 7: Adjusted control strategy for implementation of air as an additional heat source in summer to reduce investment costs.

4.2 Results for System with AHP Addition

With this adapted system configuration, the system was again simulated and optimized for the lowest levelized cost of heat. The optimization resulted in a significant reduction of the solar thermal collector field to 4,000 m² in combination with 200 kWp PV. The PV size was not optimized but set according to the available land area and on basis of the heat pump's capacity. With this combination the seasonal storage can be completely filled in summer, while the winter load is still fully covered. Since the solar thermal gains during winter are small compared to the heat demand, the effect in winter is negligible.

Figure 8 shows the resulting monthly energy balance together with the annual shares of the different heat sources covering the total heat demand of the DHN. Solar thermal remains the dominant heat source, contributing 75 %

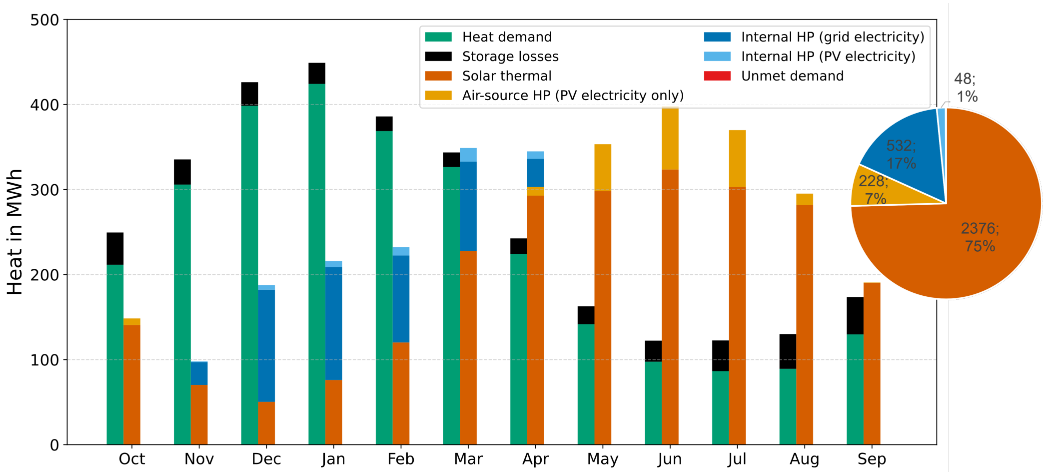

Fig. 8: Energy balances and solar fraction for the system configuration with 4,000 m² evacuated-tube collectors and a 770 kW_{th} internal heat pump, which can be additionally used to charge the seasonal storage during summer with ambient air as heat source.

(2,400 MWh/a) of the annual heat supply, while the internal heat pump operated with grid electricity in winter covers a further 17 % (530 MWh/a). The heat pump operated with ambient air as heat source and PV electricity contributes an additional 7 % (230 MWh/a) between May and September, and the internal heat pump running on PV electricity adds the remaining 1 % (50 MWh/a); unmet demand stays negligible throughout the year. The two heat sources complement each other well during summer: whenever PV electricity is available, the heat pump uses ambient air to raise the temperature of the lower part of the seasonal storage to an intermediate level, while the solar thermal collectors, which can reach substantially higher temperatures, are used to charge the upper, hotter part of the storage. Although this preheating slightly increases the return temperature to the collector field and therefore somewhat reduces its efficiency, the overall effect is still favorable, since the same temperature lift would otherwise have to be provided by the heat pump using additional (grid) electricity with a decreased COP.

4.3 Cost Reduction and Break-Even-Point

The integration of air as an additional heat source for the internal heat pump allows for a significant reduction in the size of the solar thermal collector field by 1,500 m^2. This subsequently reduces the investment costs for the collector field depending on the specific costs for the collector field. With mean specific costs for evacuated-tube collector of 550 EUR/m^2, this results in a cost reduction of approximately 825,000 EUR. Of course, to integrate air as a heat source into the existing system, an additional fluid loop and an air-water heat exchanger are needed. The additional investment costs are calculated based on the following assumptions: The necessary cooling capacity of the air-water heat exchanger is estimated at 616 kW_{th} (approximately 80 % of the heat pump's nominal heating capacity); Specific costs for the air-water heat exchanger are assumed to be 260 EUR/kW_{th}; An additional factor of 1.5 is applied to account for fluid, piping, pumps, and control system. Since the heat pump capacity is fixed at 770 kW_{th}, the additional investment costs for the air-water heat exchanger are estimated at approximately 240,000 EUR. Additionally, the specific PV costs are estimated at 800 EUR/kWp, resulting in additional investment costs of 160,000 EUR for the 200 kWp PV field.

For the fixed cost assumptions above, 425,000 EUR of investment costs can be saved by integrating air as an additional heat source for the internal heat pump. Moreover, since air is only used as heat source in summer and when PV electricity is available, the operational costs of the overall system are not significantly affected. With decreased investment costs and similar operational costs, the LCoH are reduced as well, resulting in an overall improvement of the economic feasibility of the system. Of course, one main parameter for this calculation is the specific cost for the solar thermal collector field. Figure 9 shows the sensitivity of resulting investment cost savings and the break-even point for the specific costs of the solar thermal collector field. As the figure shows, the AHP system configuration is economically beneficial for specific collector costs above 250 EUR/m^2, which is significantly lower than the current market prices for evacuated-tube collectors, and even for flat plate collector. Of course, the system complexity is increased and the integration of the additional heat source requires more planning, construction effort, and a more complex control strategy, but even so, the economic benefits are substantial.

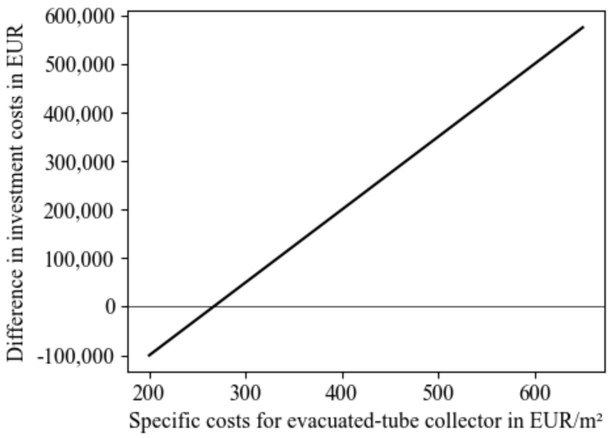

Fig. 9: Sensitivity analysis of investment cost savings for the AHP system configuration with integrated air heat source. Positive differences mean PV-AHP-supported system is less expensive and vice versa.

Although this concept could have resulted in significant investment cost savings for Rüdigheim, the option described in Section 3.3 was ultimately pursued. The advanced stage of planning and the energy cooperative's concerns about compliance with subsidy regulations due to the differences in system structure were the decisive factors here.

5. Current Construction Progress

Figure 10 shows the location of the seasonal storage and collector field before construction. The land is located on the immediate outskirts of the village and was previously used as a sports field. The small building in the photo is the current clubhouse and will remain unchanged.

Fig. 10: Location of the seasonal storage and collector field before construction.

Construction in Rüdigheim officially started in October 2025. First, the foundation for the seasonal storage was built, see Figure 11 (left). Due to a cold winter 2025/2026 concrete work was delayed initially, but the foundation was completed in February 2026. Immediately after, the storage tank construction started. The storage was built on site out of 28 tons of steel by a specialized contractor. Construction of the storage tank was completed in mid-April 2026. After that until mid-July, the insulation (400 mm) and outer shell of the storage tank was installed, see Figure 11 (right). The final storage is approximately 16 m high and measures 36 m in diameter.

Fig. 11: Foundation (left) and insulation (right) during construction of the seasonal storage tank.

Figure 12 shows the completed seasonal storage tank with the energy central in the foreground. The energy central is built as a quick-built metal hall and will house the heat pumps, the solar station, and the transfer station of the district heating network, as well as the respective peripherals, including the measurement equipment and the central controller. The foundation of the energy central was built mid July 2026, the hall itself was completed before September 2026.

Not illustrated is the current progress regarding the district heating network and the solar thermal collector field. The main pipes for both have already been laid underground on the adjacent property. The piping for the solar thermal collectors was prefabricated in Denmark and is available on site for installation. Currently (September 2026) the first main DHN pipes are laid in adjacent streets in Rüdigheim.

Fig. 12: Completed seasonal storage tank with energy central.

6. Acknowledgements

The authors would like to thank the Hesse State Ministry of Economy for long term committed support of the solar district heating project in Rüdigheim. We also thank the Federal Ministry of Economic Affairs and Energy (BMWE) for funding the accompanying scientific research (“ruralHeat”, FKZ: 03EN6031). We are furthermore grateful to the energy cooperative Sonnenwärme Rüdigheim eG for the great co-operation. We would also like to thank the companies responsible for the planning and execution, Cupasol GmbH, ratioplan GmbH, and Viessmann Deutschland GmbH.

References

Konstantinos Braimakis. Comparative techno-economic assessment of solar district heating architectures based on combined solar thermal collectors, heat pumps, pvs and batteries. *Applied Thermal Engineering*, 281: 128723, 2025. ISSN 13594311. doi: 10.1016/j.applthermaleng.2025.128723.

T. Brown, D. Schlachtberger, A. Kies, S. Schramm, and M. Greiner. Synergies of sector coupling and transmission reinforcement in a cost-optimised, highly renewable european energy system. *Energy*, 160: 720–739, 2018. ISSN 03605442. doi: 10.1016/j.energy.2018.06.222.

Buildings Performance Institute Europe. Report on the evolution of the european regulatory framework for buildings efficiency, 2022. URL `https://www.bpie.eu/publication/a-guidebook-to-european-buildings-efficiency-key-regulatory-and-policy-developments`.

Bundesamt für Wirtschaft und Ausfuhrkontrolle (BAFA). Bundesförderung für effiziente wärmenetze: technische anforderungen module 1 bis 4, 2022.

Nikolaos Damianakis, Gautham Ram Chandra Mouli, Pavol Bauer, and Yunhe Yu. Assessing the grid impact of electric vehicles, heat pumps & pv generation in dutch lv distribution grids. *Applied Energy*, 352:121878, 2023. ISSN 03062619. doi: 10.1016/j.apenergy.2023.121878.

Deutscher Bundestag. Bundes-klimaschutzgesetz vom 12. dezember 2019 (bgbl. i s. 2513), das zuletzt durch artikel 1 des gesetzes vom 15. juli 2024 (bgbl. 2024 i nr. 235) geändert worden ist": Ksg, 2019. URL `https://www.gesetze-im-internet.de/ksg/KSG`.

EU. Regulation (eu) 2021/1119 of the european parliament and of the council of 30 june 2021 establishing the framework for achieving climate neutrality and amending regulations (ec) no 401/2009 and (eu) 2018/1999 ('european climate law'). *Official Journal of the European Union L 243*, 1:64, 2021.

Norman Gerhardt. Entwicklung der gebäudewärme und rückkopplung mit dem energiesystem in -95 % thg klimazielszenarien, 2019.

Jörn Harrandt, Michael Carus, Christopher vom Berg, and Nicolas Hark. Eu and global: Biomass demand for transport fuels, aviation and shipping up to 2050 and implications for biomass supply to the chemical sector, 2025.

IEA ES Task 39. https://iea-es.org/task-39, 01.12.2025. URL `https://iea-es.org/task-39/`.

IEA ES Task 45. https://iea-es.org/task-45, 21.11.2025. URL `https://iea-es.org/task-45/`.

IEA SHC. Iea shc || international energy agency solar heating and cooling programme (iea shc) - solar heating, solar cooling, solar tasks, 03.12.2025. URL `https://www.iea-shc.org/`.

IEA SHC Task 68. Iea shc || task 68 || efficient solar district heating systems, 01.12.2025. URL `https://task68.iea-shc.org/`.

Jan Kelch, Oleg Kusyy, Johannes Zipplies, Janybek Orozaliev, and Klaus Vajen. Comparison of solar district heating and renovation of buildings as measures for decarbonization of heat supply in rural areas. *Solar Energy Advances*, 4:100060, 2024. ISSN 26671131. doi: 10.1016/j.seja.2024.100060.

Kertu Lepiksaar, Kiur Kalme, Andres Siirde, and Anna Volkova. Heat pump use in rural district heating networks in estonia. *Environmental and Climate Technologies*, 25(1):786–802, 2021. doi: 10.2478/rtuect-2021-0059.

Henrik Lund, Sven Werner, Robin Wiltshire, Svend Svendsen, Jan Eric Thorsen, Frede Hvelplund, and Brian Vad Mathiesen. 4th generation district heating (4gdh). *Energy*, 68:1–11, 2014. ISSN 03605442. doi: 10.1016/j.energy.2014.02.089.

B. V. Mathiesen, H. Lund, D. Connolly, H. Wenzel, P. A. Østergaard, B. Möller, S. Nielsen, I. Ridjan, P. Karnøe, K. Sperling, and F. K. Hvelplund. Smart energy systems for coherent 100% renewable energy and transport solutions. *Applied Energy*, 145:139–154, 2015. ISSN 03062619. doi: 10.1016/j.apenergy.2015.01.075.

Paola Pozo, Matthias Bösch, and Jörg Schweinle. Monitoring the sustainability of the eu biomass supply: A novel hybrid approach combining tracing and selected sustainability impacts. *Land*, 13(9):1366, 2024. doi: 10.3390/land13091366.

Klaudia Słomczyńska, Paweł Mirek, and Marcin Panowski. Solar heating for pit thermal energy storage – comparison of solar thermal and photovoltaic systems in trnsys 18. *Advances in Science and Technology Research Journal*, 16(5):40–51, 2022. ISSN 2080-4075. doi: 10.12913/22998624/153015.

V. M. Soltero, R. Chacartegui, C. Ortiz, and R. Velázquez. Potential of biomass district heating systems in rural areas. *Energy*, 156:132–143, 2018. ISSN 03605442. doi: 10.1016/j.energy.2018.05.051.

Dominik Steiner and Christof Lanzerstorfer. Particulate emissions from biomass power plants: a practical review and measurement uncertainty issues. *Clean Technologies and Environmental Policy*, 26(4):1039–1048, 2024. ISSN 1618-9558. doi: 10.1007/s10098-023-02645-6.

Ulrich Trabert, Jan Kelch, Janybek Orozaliev, and Klaus Vajen. Decarbonizing building stock with renewable district heating-a case study for a rural area in germany. In *Proceeding of ISES Solar World Congress 2019. IEA SHC International Conference on Solar Heating and Cooling for Building Industry 2019*, pages 470–481, 2020.

TREASURE Project. Treasure project, 21.11.2025. URL `https://www.treasure-project.eu/`.

Paul Volk, Christoph Schmelzer, Oleg Kusyy, Janybek Orozaliev, Ulrike Jordan, and Klaus Vajen. Two case studies for renewable district heating with solar fraction ≥ 70 %. In Dave Renne, editor, *EuroSun 2024*, pages 1–11, Freiburg, Germany, 2025. International Solar Energy Society. ISBN 978-3-9826306-0-1. doi: 10.18086/eurosun.2024.03.07.

Sven Werner. International review of district heating and cooling. *Energy*, 137:617–631, 2017. ISSN 03605442. doi: 10.1016/j.energy.2017.04.045.